Wnt/β-catenin Signaling Controls Maxillofacial Hyperostosis

J. Chen[1,2*], P.L. Cuevas[1*], J.S. Dworan[1,3], I. Dawid[1], H. Turkkahraman[4] (iD),
K. Tran[1], J. Delgado-Calle[5], T. Bellido[5], J.P. Gorski[6] (iD), B. Liu[1], J.B. Brunski[1],
and J.A. Helms[1] (iD)

Abstract

The roles of Wnt/β-catenin signaling in regulating the morphology and microstructure of craniomaxillofacial (CMF) bones was explored using mice carrying a constitutively active form of β-catenin in activating Dmp1-expressing cells (e.g., daβcat^{Ot} mice). By postnatal day 24, daβcat^{Ot} mice exhibited midfacial truncations coupled with maxillary and mandibular hyperostosis that progressively worsened with age. Mechanistic insights into the basis for the hyperostotic facial phenotype were gained through molecular and cellular analyses, which revealed that constitutively activated β-catenin in Dmp1-expressing cells resulted in an increase in osteoblast number and an increased rate of mineral apposition. An increase in osteoblasts was accompanied by an increase in osteocytes, but they failed to mature. The resulting CMF bone matrix also had an abundance of osteoid, and in locations where compact lamellar bone typically forms, it was replaced by porous, woven bone. The hyperostotic facial phenotype was progressive. These findings identify for the first time a ligand-independent positive feedback loop whereby unrestrained Wnt/β-catenin signaling results in a CMF phenotype of progressive hyperostosis combined with architecturally abnormal, poorly mineralized matrix that is reminiscent of craniotubular disorders in humans.

Keywords: congenital cortical hyperostosis, craniofacial abnormalities, facial bones, periosteum, craniotubular disorders, Wnt signaling pathway

Introduction

All mineralized tissues in the maxillofacial skeleton (e.g., enamel, dentin, cementum, and bone) depend in some way upon Wnt/β-catenin signaling. Using Wnt reporter and lineage-tracing strains of mice, molecular "maps" of Wnt responsiveness in mineralized tissues of the craniomaxillofacial (CMF) complex have been generated, and these demonstrate that Wnt/β-catenin signaling sites colocalize with stem/progenitor populations at the incisor apex, in the dental pulp, in cementum, in maxillofacial periostea, and in cranial sutures (Yin et al. 2015). Loss- and gain-of-function studies have demonstrated the critical nature of Wnt/β-catenin signaling in regulating the rate of alveolar bone, dentin, and cementum accumulation (Kuchler et al. 2014; Lim et al. 2014; Goes et al. 2019; Zhao et al. 2019).

Wnt signaling also influences the growth and shape of the head skeleton. From zebrafish (Parsons et al. 2014), chick (Brugmann et al. 2010), and mouse (Brault et al. 2001; Chen et al. 2021) to humans carrying mutations in Wnt pathway components (Boyden et al. 2002), it is understood that normal growth of the head skeleton requires a balance between sites of active and inactive Wnt/β-catenin signaling. Beyond this general statement, however, mechanistic insights into how Wnt/β-catenin signaling regulates both the morphogenesis and microarchitecture of the CMF skeleton are lacking. This knowledge gap is in part attributable to the fact that most studies evaluating the effects of enhanced Wnt signaling focus on

the appendicular skeleton (Boyden et al. 2002; Little et al. 2002; Clement-Lacroix et al. 2005; Li et al. 2005; Morvan et al. 2006; Bennett et al. 2007). Consequently, it is unclear how the CMF phenotypes of individuals caused by amplified Wnt/β-catenin signaling actually come about.

To address this question, we employed a genetic approach that constitutively amplified Wnt/β-catenin signaling in

[1]Division of Plastic and Reconstructive Surgery, Department of Surgery, Stanford University School of Medicine, Palo Alto, CA, USA
[2]State Key Laboratory of Oral Diseases & National Clinical Research Center for Oral Diseases, West China Hospital of Stomatology, Sichuan University, Chengdu, China
[3]Medical University of Vienna, Department of Anatomy, Center for Anatomy and Cell Biology, Vienna, Austria
[4]Indiana University School of Dentistry, Department of Orthodontics & Oral Facial Genetics, Indianapolis, IN, USA
[5]Department of Physiology & Biophysics, University of Arkansas for Medical Sciences, Little Rock, AR, USA
[6]Department of Oral and Craniofacial Sciences, School of Dentistry, and Center of Excellence in Mineralized Tissue Research, University of Missouri–Kansas City, Kansas City, MO, USA
*Authors contributing equally to this article.

A supplemental appendix to this article is available online.

Corresponding Author:
J.A. Helms, Division of Plastic and Reconstructive Surgery, Department of Surgery, School of Medicine, Stanford University, 1651 Page Mill Road, Palo Alto, CA 94305, USA.
Email: jhelms@stanford.edu

Dmp1-expressing cells. This genetic approach was adopted to circumvent the early lethality associated with many Wnt-null mutants. Dmp1 is expressed in osteocytes, odontoblasts, and cementocytes as well as their progenitors (e.g., osteoblasts, odontoblasts, and cementoblasts), beginning around embryonic day 15.5 (Feng et al. 2003). Mice expressing a dominant active form of β-catenin in Dmp1-positive osteocytes (e.g., daβcat^{Ot} mice) have no apparent skeletal anomalies at birth (Tu et al. 2015), but by postnatal day 24 (P24), a phenotype begins to emerge.

Analyses of daβcat^{Ot} mice beginning at P24 and extending to P120 demonstrated that Wnt/β-catenin signaling modulates the number of osteoblasts and density of osteocytes in CMF bone. As the number of osteoblasts increases, so, too, does the expression of Dmp1 itself, leading to a positive feedback loop that disrupts the homeostatic control of bone remodeling. Normally, bone formation is balanced by bone resorption, but in daβcat^{Ot} mice, osteoblasts produce twice as much matrix as controls and bone formation outpaces bone resorption. Although bone mass is increased in daβcat^{Ot} mice, bone quality decreases. Osteoid accumulates, osteocytes fail to mature, and where lamellar bone should form, there is instead a porous woven bone matrix. The dramatic, progressive bone accumulation in the jaw skeleton contributes to premature suture fusion and tooth ankylosis, resulting in a facial phenotype that is equivalent to that exhibited by patients with craniotubular disorders. Collectively, these data provide new insights into the roles of Wnt/β-catenin signaling in shaping the head skeleton.

Methods and Materials

Animals

Experimental protocols followed ARRIVE (Animal Research: Reporting of In Vivo Experiments) guidelines. Please see Appendix for information on how daβcat^{Ot} and Dmp1Cre$^{GFP/+}$ mice were generated and maintained.

Fluorochrome Labeling and Histomorphometric Analyses

Mice received intraperitoneal injections of calcein green and alizarin red injections to monitor the rate of mineralized matrix secretion. Details are provided in the Appendix.

Histomorphometric analyses were performed using established landmarks and established methods to produce mineral apposition rate (MAR), mineralizing surface/bone surface (MS/BS), bone formation rate/bone surface (BFR/BS), and mineral apposition rate/cellular density (MAR/CD; see Dempster et al. 2013).

Landmarking measurements (Vora et al. 2015) were carried out on micro–computed tomography (μCT) images by multiple investigators who were blinded to the genotype of the mice; values were then averaged, and standard deviations were reported.

Statistical Analyses

Results are presented as mean ± SD. Statistical analyses were performed using Prism 7.0 (GraphPad Software). Data comparisons were based on 1-way analysis of variance (ANOVA) followed by Tukey post hoc testing. Significance was attained at $*P < 0.05$, $**P < 0.01$, and $***P < 0.001$.

Please see Appendix for details on μCT analyses, sample collection, tissue processing, histology, and molecular analyses.

Results

Activated Wnt/β-catenin in DMP1-Expressing Cells Causes Maxillary and Mandibular Hyperostosis

Using Dmp1Cre$^{GFP/+}$ reporter mice, green fluorescent protein (GFP) expression in mineralized tissues of the CMF skeleton was examined. GFP staining was detected in mature osteoblasts and osteocytes, in odontoblasts, and in cementoblasts (Fig. 1A–E). The pattern of GFP in odontoblasts (Fig. 1E) was mirrored by Dmp1 immunostaining in odontoblasts (Fig. 1F), verifying fidelity of the reporter strain.

Daβcat^{Ot} mice carry an activated form of β-catenin in Dmp1-expressing cells, and consequently, the accumulation of all CMF mineralized tissues was impacted (Fig. 1G, H; Appendix Fig. 1). The daβcat^{Ot} mandible and maxilla were significantly thicker and denser than controls (Fig. 1H; Appendix Fig. 1). Dentin was also thicker, which constricted the pulp cavities, and root apices were bulbous due to the accumulation of cellular cementum (Appendix Fig. 1). In many instances, cellular cementum fused with alveolar bone and obliterated the periodontal ligament (PDL) space, which resulted in tooth ankylosis (Appendix Fig. 1).

Histomorphometric analyses were undertaken to quantitatively characterize growth alterations caused by elevated Wnt/β-catenin signaling. Anterior projection of the upper jaw was reduced because of truncations in growth of the daβcat^{Ot} premaxilla, maxilla, and palatine bone; the growth disturbance worsened over time (Fig. 1I). Anterior projection of the lower jaw was also hindered due to truncations in the corpus, ramus, and mandible (Fig. 1G–I; Appendix Fig. 1). Daβcat^{Ot} faces were also significantly wider (Appendix Fig. 1).

Sutures are growth centers in the CMF skeleton. Imaging studies demonstrated the premaxillary-maxillary suture, which typically appears as an undulating, radiolucent space between the bony fronts of the maxilla and premaxilla (Fig. 1J) and, histologically, as 2 bone fronts separated by a fibrous interzone (Fig. 1K). In daβcat^{Ot} mice, the premaxilla and maxilla coalesced, which eliminated the radiolucent suture (white box, Fig. 1L). Histologically, the fibrous interzone was reduced to a narrow band of fibrous tissue by bone overgrowth (arrowheads, Fig. 1M; quantified in Fig. 1N).

In some high bone mass diseases (e.g., osteopetrosis), the phenotype is a result of defective osteoclast activity. In daβcat^{Ot} mice, however, Tartrate-resistant acid phosphatase (TRAP)
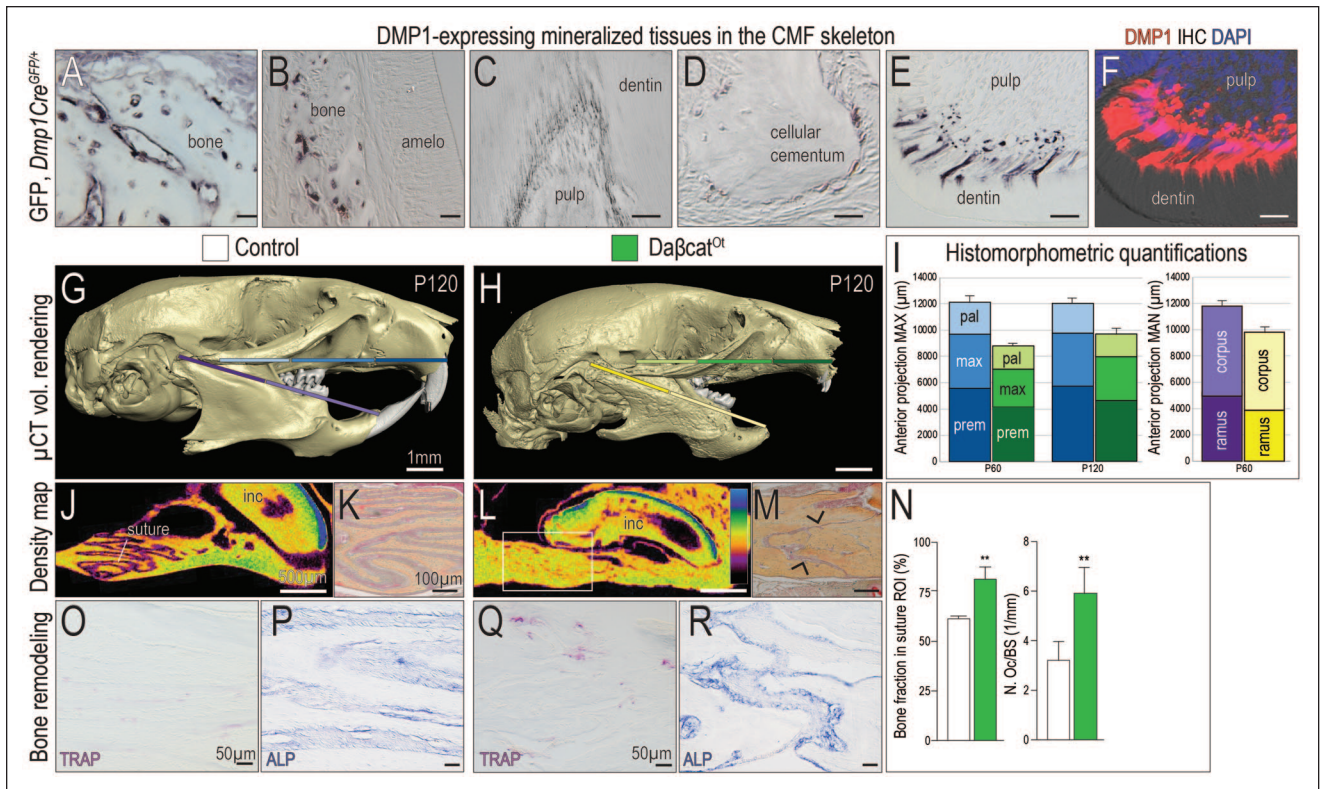
Figure 1. Maxillary and mandibular hyperostosis result from constitutive activation of Wnt/β-catenin signaling in DMP1-expressing cells. Using Dmp1Cre^{GFP/+} mice, immunostaining for green fluorescent protein (GFP) was performed in mineralized tissues of the craniomaxillofacial (CMF) skeleton, including (**A**, **B**) alveolar bone, (**C**) odontoblasts, and (**D**) cementoblasts near the tooth root apices. In near-adjacent sections, the patterns of (**E**) GFP immunostaining and (**F**) Dmp1 immunostaining are indistinguishable. Micro–computed tomography (μCT) imaging of postnatal day 120 (P120) (**G**) control and (**H**) daβcat^{Ot} mice. Colored bars correspond to (**I**) histomorphometric quantifications of the premaxilla, maxilla, palatine bones in the maxilla, and the corpus and ramus in the mandible. Density mapping of μCT sagittal sections through (**J**) control and (**L**) daβcat^{Ot} maxillae, where the thickest bone is blue and the thinnest portion is purple (see scale). Pentachrome staining of representative tissue sections through (**K**) control and (**M**) daβcat^{Ot} premaxillary-maxillary sutures. (**N**) Quantification of a region of interest (ROI) in the suture, where the percentage of bone was calculated and quantification of Tartrate-resistant acid phosphatase positive (TRAP+) osteoclasts as a function of the perimeter of bone surface. (**O**) TRAP staining and (**P**) Alkaline phosphatase (ALP) activity shown in representative tissue sections through the premaxillary suture of controls and (**Q**, **R**) and daβcat^{Ot} mice. amelo, ameloblasts; mx, maxilla; pal, palatine; po, periosteum; premx, premaxilla. Scale bars: as indicated. **P < 0.01.

activity and cathepsin K expression were detectable in the sutures and throughout the CMF skeleton (Fig. 1O, Q; quantified in Fig. 1N; Appendix Fig. 1). Equivalent results have been reported in the daβcat^{Ot} appendicular skeleton (Tu et al. 2015). Rather than a loss of osteoclast or a defect in osteoclast activity, the daβcat^{Ot} hyperostotic CMF phenotype was associated with an increase in alkaline phosphatase mineralizing activity (Fig. 1P, R).

Daβcat^{Ot} Mice Exhibit a Progressive Increase in the Number of Dmp1-Expressing Osteoblasts and Osteocytes

We gained insights into the molecular mechanisms responsible for an increase in mineralizing activity by analyzing osteocyte maturation in the daβcat^{Ot} CMF skeleton. DAPI to identify cell nuclei and trichrome to stain collagen in the extracellular matrix were used to demonstrate that the daβcat^{Ot} periosteum was significantly thicker, was more cellular, and consisted of

more proliferating cells (Fig. 2A–D; quantified in Fig. 2E; Appendix Fig. 2). Osteocyte number was also significantly increased (Fig. 2A–D; quantified in Fig. 2E).

To understand how the thicker periosteum and increased osteocyte density came about, Dmp1 and β-catenin expression were examined as a function of time. Osteocytes normally express Dmp1 and β-catenin (Fig. 2F, F′), and in daβcat^{Ot} mice, in which osteocyte number is increased by ~30%, this resulted in broader expression domains for β-catenin and Dmp1 (Fig. 2G, G′, H).

To confirm this impression, control Dmp1Cre^{GFP/+} and mutant Dmp1Cre^{GFP/+};daβcat^{Ot} mice were examined. In controls, GFP expression in osteocytes was stable between P24 and P42 (Fig. 2I, J), mirroring the pattern of Dmp1 immunostaining (Fig. 2F). In Dmp1Cre^{GFP/+};daβcat^{Ot} mutants, GFP expression was significantly increased at P24 and increased still further at P42 (Fig. 2K, L; quantified in Fig. 2M). We repeated β-catenin immunostaining in control Dmp1Cre^{GFP/+} and mutant Dmp1Cre^{GFP/+};daβcat^{Ot} mice and observed the
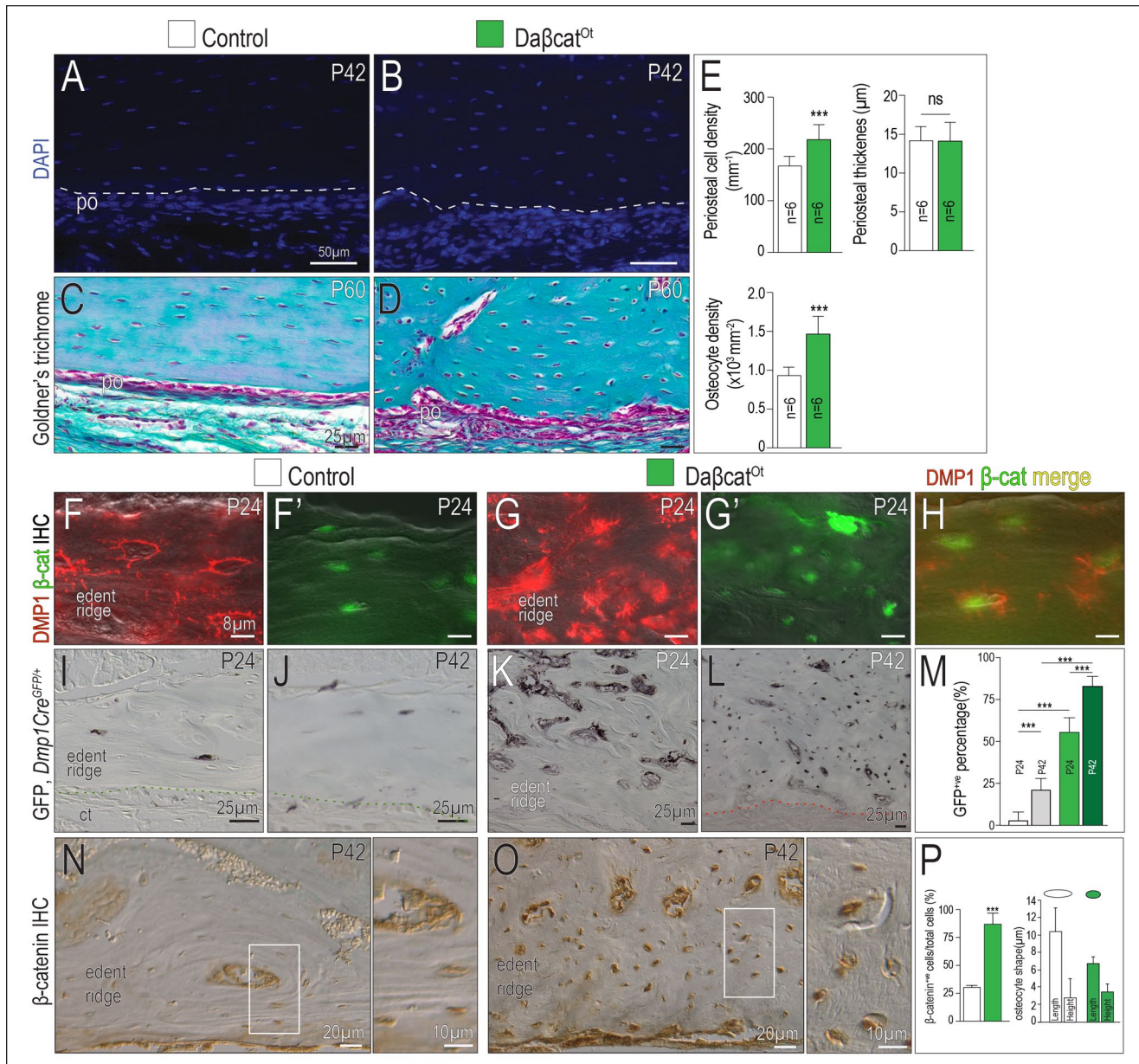
Figure 2. Dmp1-expressing osteoblasts and osteocytes are increased in daβcat^Ot craniomaxillofacial (CMF) bones. Representative sagittal tissue sections of the maxillary edentulous ridge stained with DAPI from (**A**) control and (**B**) daβcat^Ot mice. Representative tissue sections stained with Goldner's trichrome from (**C**) control and (**D**) daβcat^Ot mice. (**E**) Quantification of periosteal cell density, periosteal thickness, and osteocyte density. Coimmunostaining from (**F**) Dmp1 and (**F′**) β-catenin in controls. Coimmunostaining from (**G**) Dmp1 and (**G′**) β-catenin in daβcat^Ot mice. (**H**) Merged images of Dmp1 and β-catenin in daβcat^Ot CMF bone. Using Using Dmp1Cre^GFP/+ mice, immunostaining for GFP in (**I**) postnatal day 24 (P24) and (**J**) postnatal day 42 (P42) controls. GFP immunostaining in (**K**) P24 and (**L**) P42 daβcat^Ot mice. (**M**) Quantification of the percentage of GFP⁺ cells in a region of interest (ROI) from P24 and P42 controls (white and gray bars) and from P24 and P42 daβcat^Ot mutants (green bars). β-Catenin immunostaining on representative tissue sections from (**N**) P42 control and (**O**) daβcat^Ot mutant mice. (**P**) Quantification of β-catenin⁺ cells/total cells in a ROI and osteocyte shape, expressed as length and height of representative lacunae. Abbreviations as indicated in Fig. 1. ***$P<0.001$.

broader, stronger expression in the mutants (Fig. 2N, O; quantified in Fig. 2P). In addition to an increase in number, osteocyte morphology was altered in daβcat^Ot mice: compared to the typical elongated, flattened morphology of osteocytes in lamellar bone, daβcat^Ot osteocytes in the same anatomical location were rounded (Fig. 2O; quantified in Fig. 2P).

An Increase in Osteoblasts Is Responsible for a Higher Mineral Apposition Rate and an Accumulation of Immature Osteocytes in daβcat^Ot Mice

Dynamic histomorphometric analyses provided further mechanistic insights into the basis for the hyperostotic phenotype in

daβcat[Ot] mice. Using calcein green and alizarin red uptake, a significant increase in MAR was measured (Fig. 3A, B; quantified in Fig. 3C). When the elevated MAR was normalized to cell density, daβcat[Ot] osteoblasts produced twice as much matrix as control osteoblasts (MAR/CD; Fig. 3C).

The elevated MAR was associated with an accumulation of osteoid. In controls, unmineralized osteoid was visible as a thin seam adjacent to the mineralized matrix, but in daβcat[Ot] CMF bones, osteoid was abundant (Fig. 3D, E). Osteoid is secreted by osteoblasts, and in keeping with the excess of osteoid, the number of Runx2^{+} osteoblasts was also significantly elevated in daβcat[Ot] CMF bones (Fig. 3F, G; quantified in Fig. 3H). Runx2 and β-catenin coimmunostaining (Fig. 3I, J) along with Osterix immunostaining (Fig. 3K, L; quantified in Fig. 3M) demonstrated that osteoblast number was significantly increased in daβcat[Ot] mice. Daβcat[Ot] osteocytes continued to express Runx2 and Osterix, an indication of their immature state.

The Wnt-Dependent Increase in CMF Bone Mass Is Accompanied by a Decrease in Bone Quality

CMF bones in daβcat[Ot] mice were thicker than controls (Fig. 4A, B) and grew progressively thicker with time (Fig. 4C). While bone mass increased, density mapping illustrated that daβcat[Ot] CMF bones became progressively more porous (Fig. 4D–F; quantified in Fig. 4G). The increase in porosity was accompanied by an alteration in collagen organization: in the edentulous ridge of control mice, lamellar organization of the collagen was readily evident in pentachrome and picrosirius red–stained tissues (Fig. 4H, H′). In the same anatomical region in daβcat[Ot] mice, collagen had a basket-weave pattern (Fig. 4I, I′). The porous, disorganized collagen matrix observed in daβcat[Ot] bones bore a striking resemblance to the woven bone that typically forms after an injury (compare Fig. 4I, I′ with Fig. 4J, J′). Compared to the maturation of bone in a normal-healing maxillary defect that transitions from a porous collagen matrix to a denser one (stippled bars, Fig. 4K), the porosity in the daβcat[Ot] bones persisted (green bar, Fig. 4K). The daβcat[Ot] edentulous ridge never developed a dense lamellar organization like the control edentulous ridge (striped bar, Fig. 4K).

Discussion

Examining Craniomaxillofacial Morphogenesis to Understand Hyperostotic Facial Phenotypes

In this study, we focused on the consequences of amplified Wnt/β-catenin signaling in the CMF skeleton. Most studies that evaluate the effects of enhanced Wnt signaling on bone formation focus on the appendicular skeleton (Boyden et al. 2002; Little et al. 2002; Clement-Lacroix et al. 2005; Li et al. 2005; Morvan et al. 2006; Bennett et al. 2007), in large part because of the relatively simple geometry and growth pattern of tubular bones. Tubular bones elongate unidirectionally at

their epiphyses, but within the jaw skeleton, growth patterns are far more complex. The maxilla grows entirely by intramembranous ossification, while the mandible grows anteriorly by endochondral ossification at the condyle, vertically by intramembranous ossification at the corpus and ramus, and mediolaterally by a combination of endochondral ossification at the symphysis and intramembranous ossification in the corpus and ramus. So while the growth pattern of long bones gives us clues as to what we might anticipate finding in the facial structures, they are inadequate to understand the more complex and unique nature of CMF growth and morphogenesis.

Hyperostotic Facial Phenotypes Are Associated with Abnormally High Wnt Signaling

Craniotubular disorders, as the name implies, affect both CMF and appendicular bones, but these are rare conditions and have variable degrees of phenotypic expression; consequently, there is a limited understanding of the basis for most facial hyperostotic phenotypes. Recently, a number of groups have addressed this knowledge gap, through analyses of mice carrying mutations similar to those identified in patients with craniometaphyseal dysplasia (CMD; Dutra et al. 2013), osteopathia striata with cranial sclerosis (OSCS; Comai et al. 2018), and van Buchem disease (Chen et al. 2021).

We submit that the daβcat[Ot] CMF phenotype shares multiple similarities with the most severe craniotubular disorders. For example, a consistent feature of craniotubular disorders is thickened, sclerotic facial bones that manifest in early childhood and grow progressively more severe with time (Gorlin et al. 1990). This is an apt description of the daβcat[Ot] CMF skeleton (Fig. 1; Appendix Fig. 1; Fig. 4).

In some cases, the genetic basis for a craniotubular disorder has been identified: van Buchem disease is due to inactivating mutations in the WNT inhibitor, sclerostin (Loots et al. 2005), and OSCS is caused by heterozygous deletions in AMER1/WTX (Jenkins et al. 2009). Both types of mutations are predicted to result in enhanced WNT signaling. In the case of sclerostin, loss-of-function mutations result in ligand-dependent amplification in WNT signaling. AMER/WTX normally interacts with β-catenin to repress Wnt signaling (Tanneberger et al. 2011), but in patients with heterozygous mutations in AMER/WTX, β-catenin is not degraded and instead translocates to the nucleus, where it increases transcription of WNT target genes (Jenkins et al. 2009).

Our findings provide further evidence linking hyperostotic CMF phenotypes to amplified Wnt/β-catenin signaling. In a previous study, we evaluated the CMF consequences of elevated Wnt signaling caused by functional deletion of sclerostin (Chen et al. 2021). The murine phenotype closely aligned with the facial phenotype observed in patients with SOST mutations/van Buchem disease (Van Buchem et al. 1962), but compared to the daβcat[Ot] phenotype shown here, the *Sost^{-/-}* CMF phenotype is relatively mild: while both *Sost^{-/-}* and daβcat[Ot] CMF bones are both significantly thicker, and MARs are significantly higher than controls, only in daβcat[Ot] mice are
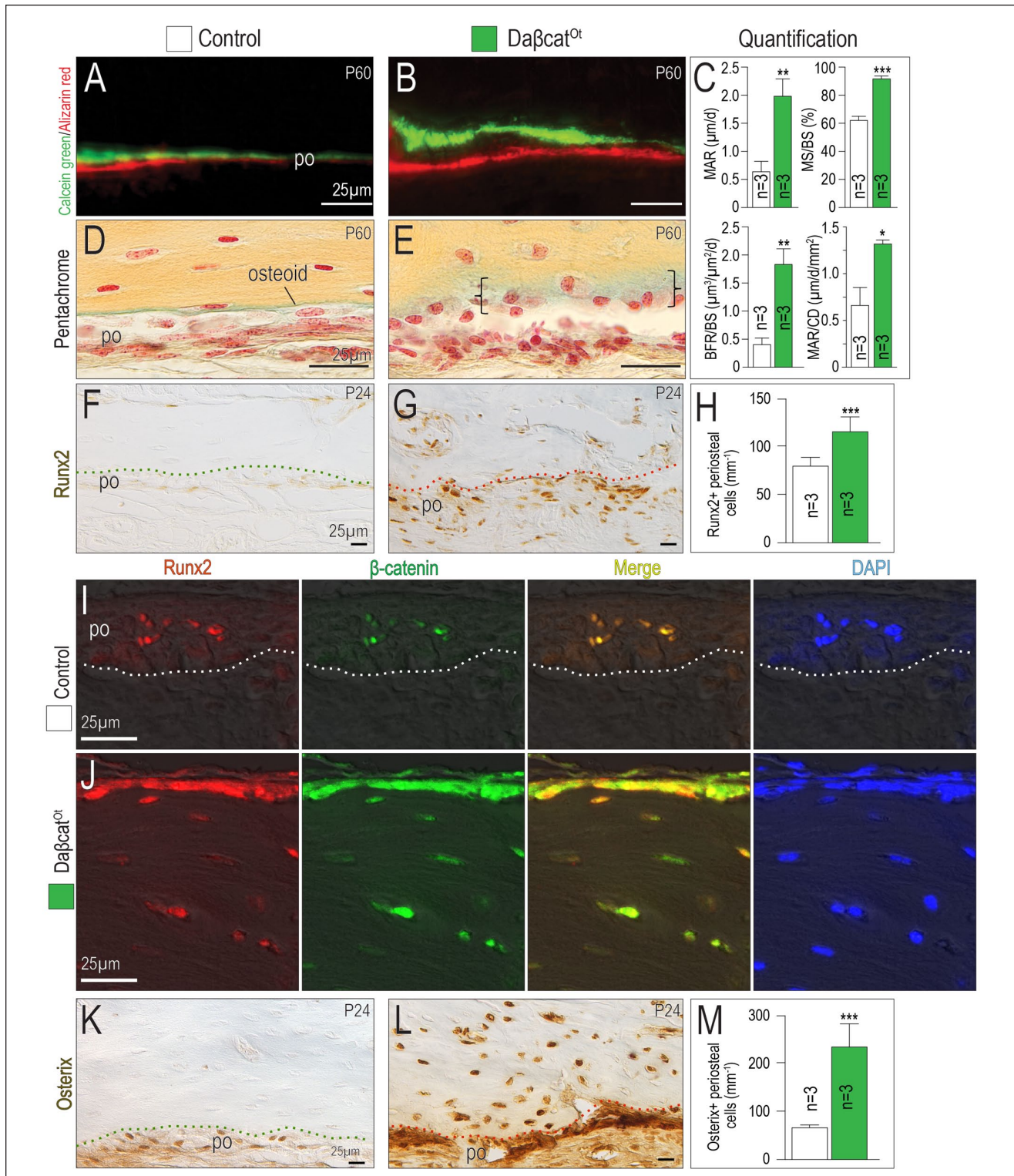
Figure 3. Accelerated mineral apposition rate and an accumulation of immature osteocytes result from constitutively activated Wnt/β-catenin signaling. Representative sections of calcein green– and alizarin red–labeled bone in the maxillary edentulous ridges in (**A**) control and (**B**) daβcat[Ot] mice. (**C**) Quantification of dynamic histomorphometric indices including mineral apposition rate (MAR), mineralizing surface over bone surface (MS/BS), bone formation rate over bone surface (BFR/BS), and mineral apposition rate over cell density (MAR/CD). Pentachrome-stained tissue sections used to visualize osteoid (green color) in (**D**) control and (**E**) daβcat[Ot] mice. Runx2 immunostaining in the maxillary edentulous ridges in (**F**) control and (**G**) daβcat[Ot] mice. (**H**) Quantification of Runx2^{+} cells in the maxillary edentulous ridge periosteum. Coimmunostaining for Runx2 (red) and β-catenin (green) in (**I**) control and (**J**) daβcat[Ot] mice. Yellow represents the merged image and DAPI (blue) identifies viable cell nuclei. Osterix immunostaining in the maxillary edentulous ridges in (**K**) control and (**L**) daβcat[Ot] mice. (**M**) Quantification of Osterix^{+} cells in the maxillary edentulous ridge periosteum. Abbreviations: as in previous figures. *$P < 0.05$. **$P < 0.01$. ***$P < 0.001$.
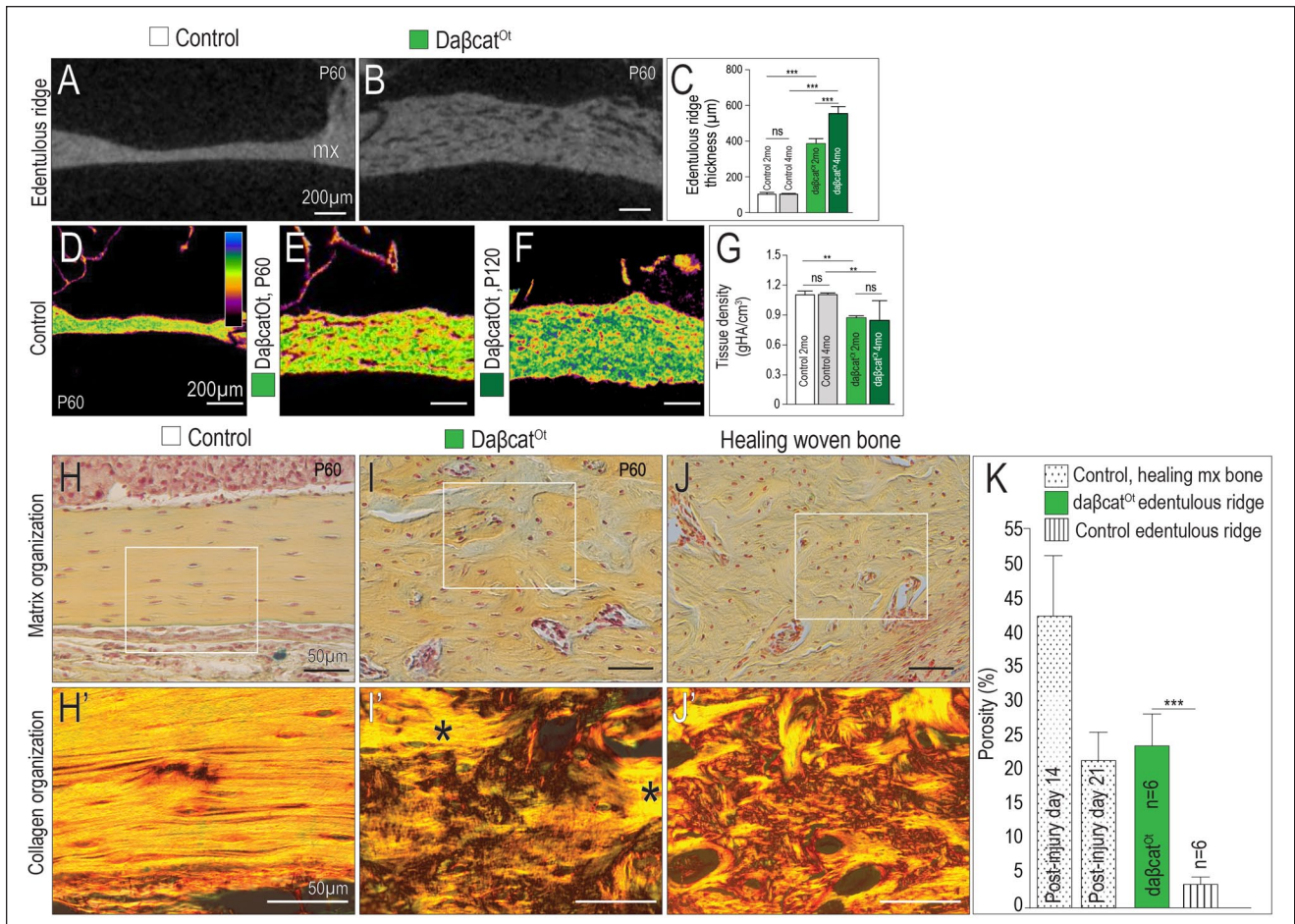
Figure 4. Constitutively activated Wnt/β-catenin signaling transforms lamellar into woven bone. Representative sagittal micro–computed tomography (μCT) sections through the maxillary edentulous ridge of (**A**) control and (**B**) daβcat[Ot] mice. (**C**) Quantification of edentulous ridge thickness. Density mapping of μCT sagittal sections through (**D**) control (P60), (**E**) daβcat[Ot] mice at postnatal day 60 (P60), and (**F**) daβcat[Ot] mice at postnatal day 120 (P120). (**G**) Quantification of tissue density as determined by μCT analysis. Pentachrome staining and picrosirius red staining of representative sagittal tissue sections, viewed under polarized light to visualize collagen fiber orientation in the maxillary edentulous ridges of (**H, H′**) controls, (**I, I′**) daβcat[Ot] mice (asterisks indicate islands of lamellar bone surrounded by woven bone), and (**J, J′**) healing maxillary bone from a wild-type mouse. (**K**) Quantification of porosity in bone as a function of injury and genotype. ns, not significant. **$P < 0.01$. ***$P < 0.001$.

osteoblast and osteocyte numbers increased. In addition, daβcat[Ot] osteoblasts produce significantly more matrix than control osteoblasts (Fig. 2E), but bone quality suffers as a consequence. The accumulation of osteoid is a hallmark of the daβcat[Ot] phenotype, and the same histological descriptions have been made of CMF bones from patients with craniotubular disorders (Welford 1959; Bjorvatn et al. 1979; Gorlin et al. 1990).

In a genetic twist of fate, daβcat[Ot] mice have more osteoblasts and osteocytes, and both populations express Dmp1 (Figs. 2, 3). By virtue of the Dmp1Cre driver, these new osteoblasts and osteocytes also express the constitutively active form β-catenin, leading to a positive feedback loop that disrupted homeostatic control of bone remodeling; this is the basis for the dramatic and progressive worsening of the hyperostotic daβcat[Ot] facial phenotype. This unique feedback loop and its resulting effects on facial hyperostosis align with the progressive nature of most human craniotubular disorders.

While it is highly unlikely that any craniotubular disorder is due to the conditional expression of an activated form of β-catenin in Dmp1-expressing cells, it should be noted that a growing number of hyperostotic disorders are indirectly associated with aberrant activation of β-catenin (Brance et al. 2020). Consequently, a detailed understanding of the daβcat[Ot] phenotype may shed light on the molecular basis for the most severe craniotubular disorders.

Understanding the Unique Facial Features of Craniotubular Disorders via Analysis of the daβcat[Ot] Facial Growth

In daβcat[Ot] mice, a flattened midface can be traced back to a disruption in growth at the facial sutures. Sutures act as growth centers, where 2 bony fronts expand by appositional growth (Persson 1995). In daβcat[Ot] mice, Runx2[+ve] osteoblasts are in

abundance, and they secrete a collagenous woven bone matrix at an abnormally high rate (Fig. 3). This accelerated rate of mineral apposition reduces/eliminates the fibrous interzone that lies between in sutures, thereby arresting any further anterior growth at the suture (Fig. 1).

daβcat^{Ot} mice have significantly wider faces (Appendix Fig. 1), which in many ways resembles the facial alterations seen in patients with van Buchem, CMD, sclerosteosis, and OSCS (Gorlin et al. 1990). Upper and lower jaws widen via appositional/intramembranous ossification, and our molecular analyses pinpoint the mechanism(s) underlying this pathological accrual: in daβcat^{Ot} mice, a pathological increase in osteoblast/osteocyte numbers (Fig. 2) is accompanied by an accelerated rate of collagen secretion and mineralization (Fig. 3).

Regulation of the Balance between Lamellar versus Woven Bone by Wnt/β-catenin Signaling

The CMF skeleton comprises both compact and cancellous bone, and differences in porosity allow for a morphological distinction between the two (Currey 1984). In daβcat^{Ot} mice, there was no clear delineation between compact and cancellous bone (Appendix Fig. 1, Fig. 2). The structural organization of bone into compact and cancellous structures is influenced by the rate at which osteoblasts secrete collagen: lamellar bone forms from osteoblasts, whose rate of collagen secretion is low (Moreira et al. 2019), and it is thought that this slow rate of secretion allows for alignment of the collagen fiber along lines of stress (Gorski 1998). Cancellous (woven) bone, on the other hand, is produced by osteoblasts whose rate of collagen secretion is higher (Gorski 1998); it is thought that because it forms quickly, the collagen fibril orientation appears to be random (Gorski 1998). In daβcat^{Ot} mice, areas of the facial skeleton that typically comprise lamellar bone appeared as woven bone (Fig. 4), and proteins that were typically expressed at low levels in lamellar bone and high levels in woven bone were strongly expressed in daβcat^{Ot} bones (Fig. 3). In keeping with the high rate of bone deposition, daβcat^{Ot} osteocytes were rounded and continued to express Runx2 and Osterix, demonstrating their immature state.

Conclusions

Data shown here support a model whereby constitutive activation of Wnt/β-catenin signaling in Dmp1-expressing cells is a key factor in determining osteoblast number and mineral apposition rate. An increase in osteoblasts was accompanied by an increase in osteocytes, but they failed to mature. The resulting CMF bone matrix had an abundance of osteoid, and in locations where compact lamellar bone typically forms, it was replaced by porous, woven bone. The hyperostotic facial phenotype was progressive. Based on phenotypic similarities and histological equivalencies, we propose that elevated Wnt/β-catenin signaling is a shared feature of craniotubular disorders in humans.

Author Contributions

J. Chen, P.L. Cuevas, contributed to conception, design, data acquisition, analysis, and interpretation, drafted and critically revised the manuscript; J.S. Dworan, I. Dawid, H. Turkkahraman, K. Tran, J.P. Gorski, B. Liu, J.B. Brunski, contributed to data acquisition, analysis, and interpretation; J. Delgado-Calle, T. Bellido, contributed to conception, design, data acquisition, analysis, and interpretation, critically revised the manuscript; J.A. Helms, contributed to conception, design, data analysis, and interpretation, drafted and critically revised the manuscript. All authors gave final approval and agree to be accountable for all aspects of the work.

Declaration of Conflicting Interests

Funding

ORCID iDs

H. Turkkahraman https://orcid.org/0000-0001-9052-7700

J.P. Gorski https://orcid.org/0000-0002-4452-6704

J.A. Helms https://orcid.org/0000-0002-0463-396X

References

Bennett CN, Ouyang H, Ma YL, Zeng Q, Gerin I, Sousa KM, Lane TF, Krishnan R, Hankenson KD, MacDougald OA. 2007. Wnt10b increases postnatal bone formation by enhancing osteoblast differentiation. J Bone Miner Res. 22(12):1924–1932.

Bjorvatn K, Gilhuus-Moe O, Aarskog D. 1979. Oral aspects of osteopetrosis. Scand J Dent Res. 87(4):245–252.

Boyden LM, Mao J, Belsky J, Mitzner L, Farhi A, Mitnick MA, Wu D, Insogna K, Lifton RP. 2002. High bone density due to a mutation in LDL-receptor-related protein 5. N Engl J Med. 346(20):1513–1521.

Brance ML, Brun LR, Coccaro NM, Aravena A, Duan S, Mumm S, Whyte MP. 2020. High bone mass from mutation of low-density lipoprotein receptor-related protein 6 (LRP6). Bone. 141:115550.

Brault V, Moore R, Kutsch S, Ishibashi M, Rowitch DH, McMahon AP, Sommer L, Boussadia O, Kemler R. 2001. Inactivation of the (β)-catenin gene by Wnt1-Cre-mediated deletion results in dramatic brain malformation and failure of craniofacial development. Development. 128(8):1253–1264.

Brugmann SA, Powder KE, Young NM, Goodnough LH, Hahn SM, James AW, Helms JA, Lovett M. 2010. Comparative gene expression analysis of avian embryonic facial structures reveals new candidates for human craniofacial disorders. Hum Mol Genet. 19(5):920–930.

Chen J, Yuan X, Pilawski I, Liu X, Delgado-Calle J, Bellido T, Turkkahraman H, Helms JA. 2021. Molecular basis for craniofacial phenotypes caused by sclerostin deletion. J Dent Res. 100(3):310–317.

Clement-Lacroix P, Ai M, Morvan F, Roman-Roman S, Vayssiere B, Belleville C, Estrera K, Warman ML, Baron R, Rawadi G. 2005. Lrp5-independent activation of wnt signaling by lithium chloride increases bone formation and bone mass in mice. Proc Natl Acad Sci U S A. 102(48):17406–17411.

Comai G, Boutet A, Tanneberger K, Massa F, Rocha AS, Charlet A, Panzolini C, Jian Motamedi F, Brommage R, Hans W, et al. 2018. Genetic and molecular insights into genotype-phenotype relationships in osteopathia striata with cranial sclerosis (OSCS) through the analysis of novel mouse Wtx mutant alleles. J Bone Miner Res. 33(5):875–887.

Currey J. 1984. Comparative mechanical properties and histology of bone. Am Zool. 24(1):5–12.

Dempster DW, Compston JE, Drezner MK, Glorieux FH, Kanis JA, Malluche H, Meunier PJ, Ott SM, Recker RR, Parfitt AM. 2013. Standardized nomenclature, symbols, and units for bone histomorphometry: a 2012 update of the report of the ASBMR histomorphometry nomenclature committee. J Bone Miner Res. 28(1):2–17.

Dutra EH, Chen IP, Reichenberger EJ. 2013. Dental abnormalities in a mouse model for craniometaphyseal dysplasia. J Dent Res. 92(2):173–179.

Feng JQ, Huang H, Lu Y, Ye L, Xie Y, Tsutsui TW, Kunieda T, Castranio T, Scott G, Bonewald LB, et al. 2003. The dentin matrix protein 1 (Dmp1) is specifically expressed in mineralized, but not soft, tissues during development. J Dent Res. 82(10):776–780.

Goes P, Dutra C, Losser L, Hofbauer LC, Rauner M, Thiele S. 2019. Loss of Dkk-1 in osteocytes mitigates alveolar bone loss in mice with periodontitis. Front Immunol. 10:2924.

Gorlin RJ, Cohen MM, Levin LS. 1990. Syndromes of the head and neck. New York (NY): Oxford University Press.

Gorski JP. 1998. Is all bone the same? Distinctive distributions and properties of non-collagenous matrix proteins in lamellar vs. woven bone imply the existence of different underlying osteogenic mechanisms. Crit Rev Oral Biol Med. 9(2):201–223.

Jenkins ZA, van Kogelenberg M, Morgan T, Jeffs A, Fukuzawa R, Pearl E, Thaller C, Hing AV, Porteous ME, Garcia-Minaur S, et al. 2009. Germline mutations in WTX cause a sclerosing skeletal dysplasia but do not predispose to tumorigenesis. Nat Genet. 41(1):95–100.

Kuchler U, Schwarze UY, Dobsak T, Heimel P, Bosshardt DD, Kneissel M, Gruber R. 2014. Dental and periodontal phenotype in sclerostin knockout mice. Int J Oral Sci. 6(2):70–76.

Li X, Zhang Y, Kang H, Liu W, Liu P, Zhang J, Harris SE, Wu D. 2005. Sclerostin binds to LRP5/6 and antagonizes canonical Wnt signaling. J Biol Chem. 280(20):19883–19887.

Lim WH, Liu B, Hunter DJ, Cheng D, Mah SJ, Helms JA. 2014. Downregulation of Wnt causes root resorption. Am J Orthod Dentofacial Orthop. 146(3):337–345.

Little RD, Carulli JP, Del Mastro RG, Dupuis J, Osborne M, Folz C, Manning SP, Swain PM, Zhao SC, Eustace B, et al. 2002. A mutation in the LDL receptor-related protein 5 gene results in the autosomal dominant high-bone-mass trait. Am J Hum Genet. 70(1):11–19.

Loots GG, Kneissel M, Keller H, Baptist M, Chang J, Collette NM, Ovcharenko D, Plajzer-Frick I, Rubin EM. 2005. Genomic deletion of a long-range bone enhancer misregulates sclerostin in van Buchem disease. Genome Res. 15(7):928–935.

Moreira CA, Dempster DW, Baron R. 2019. Anatomy and ultrastructure of bone—histogenesis, growth and remodeling. South Dartmouth (MA): MDText.com; [accessed 2021 Jan 12]. https://www.ncbi.nlm.nih.gov/books/NBK279149/.

Morvan F, Boulukos K, Clement-Lacroix P, Roman Roman S, Suc-Royer I, Vayssiere B, Ammann P, Martin P, Pinho S, Pognonec P, et al. 2006. Deletion of a single allele of the Dkk1 gene leads to an increase in bone formation and bone mass. J Bone Miner Res. 21(6):934–945.

Parsons KJ, Trent Taylor A, Powder KE, Albertson RC. 2014. Wnt signalling underlies the evolution of new phenotypes and craniofacial variability in Lake Malawi cichlids. Nat Commun. 5:3629.

Persson M. 1995. The role of sutures in normal and abnormal craniofacial growth. Acta Odontol Scand. 53(3):152–161.

Tanneberger K, Pfister AS, Kriz V, Bryja V, Schambony A, Behrens J. 2011. Structural and functional characterization of the Wnt inhibitor APC membrane recruitment 1 (Amer1). J Biol Chem. 286(22):19204–19214.

Tu X, Delgado-Calle J, Condon KW, Maycas M, Zhang H, Carlesso N, Taketo MM, Burr DB, Plotkin LI, Bellido T. 2015. Osteocytes mediate the anabolic actions of canonical Wnt/β-catenin signaling in bone. Proc Natl Acad Sci U S A. 112(5):E478–E486.

Van Buchem FS, Hadders HN, Hansen JF, Woldring MG. 1962. Hyperostosis corticalis generalisata. Report of seven cases. Am J Med. 33:387–397.

Vora SR, Camci ED, Cox TC. 2015. Postnatal ontogeny of the cranial base and craniofacial skeleton in male C57BL/6J mice: a reference standard for quantitative analysis. Front Physiol. 6:417.

Welford NT. 1959. Facial paralysis associated with osteopetrosis (marble bones); report of a case of the syndrome occurring in five generations of the same family. J Pediatr. 55(1):67–72.

Yin X, Li J, Salmon B, Huang L, Lim WH, Liu B, Hunter DJ, Ransom RC, Singh G, Gillette M, et al. 2015. Wnt signaling and its contribution to craniofacial tissue homeostasis. J Dent Res. 94(11):1487–1494.

Zhao Y, Yuan X, Bellido T, Helms JA. 2019. A correlation between Wnt/beta-catenin signaling and the rate of dentin secretion. J Endod. 45(11):1357–1364.e1.